Current Medical Science
DOI https://doi.org/10.1007/s11596-021-2360-z
41(2):398-404,2021

Fully Automatic Scar Segmentation for Late Gadolinium Enhancement MRI Images in Left Ventricle with Myocardial Infarction*

Zheng-hong WU[1†], Li-ping SUN[2†], Yun-long LIU[3], Dian-dian DONG[3], Lv TONG[3], Dong-dong DENG[3#], Yi HE[4, 5], Hui WANG[4], Yi-bo SUN[2], Jian-zeng DONG[2, 4], Ling XIA[1#]
[1]*College of Biomedical Engineering & Instrument Science, Zhejiang University, Hangzhou 310027, China*
[2]*Department of Cardiology, the First Affiliated Hospital of Zhengzhou University, Zhengzhou 450052, China*
[3]*School of Biomedical Engineering, Dalian University of Technology, Dalian 116024, China*
[4]*Department of Cardiology, Beijing Anzhen Hospital, Capital Medical University and National Clinical Research Center for Cardiovascular Diseases, Beijing 100029, China*
[5]*Department of Cardiology, Beijing Friendship Hospital, Capital Medical University, Beijing 100050, China*

Summary: Numerous methods have been published to segment the infarct tissue in the left ventricle, most of them either need manual work, post-processing, or suffer from poor reproducibility. We proposed an automatic segmentation method for segmenting the infarct tissue in left ventricle with myocardial infarction. Cardiac images of a total of 60 diseased hearts (55 human hearts and 5 porcine hearts) were used in this study. The epicardial and endocardial boundaries of the ventricles in every 2D slice of the cardiac magnetic resonance with late gadolinium enhancement images were manually segmented. The subsequent pipeline of infarct tissue segmentation is fully automatic. The segmentation results with the automatic algorithm proposed in this paper were compared to the consensus ground truth. The median of Dice overlap between our automatic method and the consensus ground truth is 0.79. We also compared the automatic method with the consensus ground truth using different image sources from different centers with different scan parameters and different scan machines. The results showed that the Dice overlap with the public dataset was 0.83, and the overall Dice overlap was 0.79. The results show that our method is robust with respect to different MRI image sources, which were scanned by different centers with different image collection parameters. The segmentation accuracy we obtained is comparable to or better than that of the conventional semi-automatic methods. Our segmentation method may be useful for processing large amount of dataset in clinic.
Key words: myocardial infarction; cardiac magnetic resonance with late gadolinium enhancement; automatic scar segmentation

Zheng-hong WU, E-mail: wzhuestc@126.com; Li-ping SUN, E-mail: lipng_18@hotmail.com
†These authors contributed equally to this study.
#Corresponding authors, Dong-dong DENG, E-mail: dengdongdong@dlut.edu.cn; Ling XIA, E-mail: xialing@zju.edu.cn
*This work was supported by the National Key Research and Development Program of China (No. 2016YFC1301002 to Jianzeng Dong), the National Natural Science Foun dation of China (No. 81901841 to Dongdong Deng, No. 81671650 and No. 81971569 to Yi He, No. 61527811 to Ling Xia), and the Key Research and Development Program of Zhejiang Province (No. 2020C03016 to Ling Xia). Dongdong Deng also acknowledges support from Dalian University of Technology (No. DUT18RC(3)068).
Electronic supplementary material The online version of this article (https://doi.org/10.1007/s11596-021-2360-z) contains supplementary material, which is available to authorized users.

Myocardial infarction (MI), a condition characterized by reduced viability of cardiac myocardium due to insufficient blood supply, is a leading cause of lethal ventricular tachyarrhythmia (VT) worldwide[1]. The presence of MI has an important prognostic and therapeutic value as a strong predictor of left ventricle remodeling and cardiac dysfunction[2]. Cardiac magnetic resonance with late gadolinium enhancement (CMR-LGE) has quickly become the standard imaging method for the identification of MI in the ventricle[3, 4]. In the CMR-LGE images, the normal myocardium is represented by low signal intensity because of the fast gadolinium wash in and wash out, whereas the infarcted tissue is represented by high signal intensity. Experimental studies have shown that the contrast distribution accurately reflects pathology of myocardium[5].

CMR-LGE has become the gold standard for

assessing the location, transmurality, and composition of MI[6, 7]. Although it is a powerful tool to visualize the complexity of the MI structure, it does not provide insight into the electrical activity of the heart, particularly the location of the VT reentrant circuits. Recently, computational modeling of hearts with ischemic cardiomyopathy has emerged as a promising tool to guide patient-specific diagnosis and the treatment of associated rhythm disorders[8–10]. This patient-specific computational modeling method needs accurate reconstruction of myocardial scar geometry so as to predict the risk of arrhythmia and the locations of re-entrant circuits in patients hearts[9, 11].

There are numerous published methods for segmenting infarct tissues in the left ventricle. The most frequently used techniques are threshold-based, such as the full-width at half-maximum[12] and the n-standard deviations[13]. Yet these methods need manual work and poor reproducibility, and their segmentation results are not ideal. Several semi-automatic or automatic methods have been proposed[14, 15], most of which need manual work or post-processing, thereby hindering efficient image processing for a large number of patients. This study aims to propose an automatic and accurate segmentation method for segmenting the infarct tissue in left ventricle with MI.

1 MATERIALS AND METHODS

1.1 Data Acquisition Database

This study used cardiac images from a total of 60 diseased hearts. Three human and five porcine datasets were collected from the website Cardiac Atlas Challenge http://www.cardiacatlas.org/challenges/ventricular-infarct-segmentation/. The human data (n=3) were from randomly selected patients who had a known history of ischemic cardiomyopathy and were under assessment for an implantable cardioverter defibrillator. The porcine data (n=5) were randomly selected from an experimental database of a pre-clinical model of chronic myocardial ischemia, with induced lesions obtained by occluding either the left-anterior descending or left-circumflex artery. The detailed information regarding image acquisition and segmentation can be found in the previous published literature[14].

The rest 52 patients were collected from Anzhen Hospital and the First Affiliated Hospital of Zhengzhou University, and this study was approved by the Institutional Review Board of Beijing Anzhen Hospital and the First Affiliated Hospital of Zhengzhou University. Informed consents were obtained from all the participants. The detailed image acquisition protocol can be found in the previous published literature[16]. Briefly, cardiac magnetic resonance scans were performed on a 1.5T scanner (Siemens Sonata 1.5T, Germany) with chest ECG gating and breathhold techniques. Contrast agent was injected via ulnar vein under high pressure, and the late imaging was performed 15 min after the injection. The scanning layer thickness was 8 mm or 10 mm with FOV between 320 mm × 320 mm and 340 mm × 340 mm. The final in-plane image resolution was between 1.4 mm and 1.75 mm.

1.2 Image Processing Pipelines

All analyses and measurements were carried out using custom software developed in Matlab (Mathwords Inc., USA). The epicardial and endocardial boundaries of the ventricles in every 2D slice of the CMR-LGE images were manually segmented by two experienced experts. The papillary muscles were excluded from the endocardium. The subsequent steps were completely automatic, summarized as follows.

Step 1: a classification method based on Gaussian mixture model (GMM) was used to segment the tissue inside the epi- and endo-cardium boundaries[17, 18]. The GMM assumes a Gaussian distribution of the image intensity of each category of tissue, where each category has its own mean intensity and variance. The GMM method classifies the tissue into different categories by optimally fitting the image histogram based on employing an expectation-maximization approach. The outcome of the final classified image was obtained by assigning each pixel to its most likely category (fig. 1A). The final segmented tissues included three different categories which were non-infarct tissue, gray zone and core scar. On the other hand, we tested the GMM method to get two different categories that included non-infarct and infarct tissue (the 2nd column in fig. 1B).

Step 2: the maximal component in each layer and the components with pixels more than M% of the maximal components were kept. The number M can be any number. We chose M=50 in this study because we found this number yielded optimal results (the 3rd column in fig. 1B).

Step 3: the connected components in each layer were calculated, and the components with bigger than N pixels were assigned as the final infarct tissue. The number N can be any number, we choose 15 in this study because we found this number could get the best results (4th column in fig. 1B).

Step 4: In order to further segment the infarct tissue detected by the GMM-based classification method into gray zone and core scar, the maximal ($intersity_{max}$) and minimal ($intersity_{min}$) values of the pixels in the infarct tissue were calculated, then the pixels > ($intersity_{max}$ –$intersity_{min}$)×$Value_{threshold}$ were assigned as core scar, and the rest pixels in the infarct area were assigned as gray zone. The $Value_{threshold}$ was chosen from 10% to 50% with 5% interval.

1.3 Evaluation Metrics for Segmentation

After analysis of the entire stack of ventricular

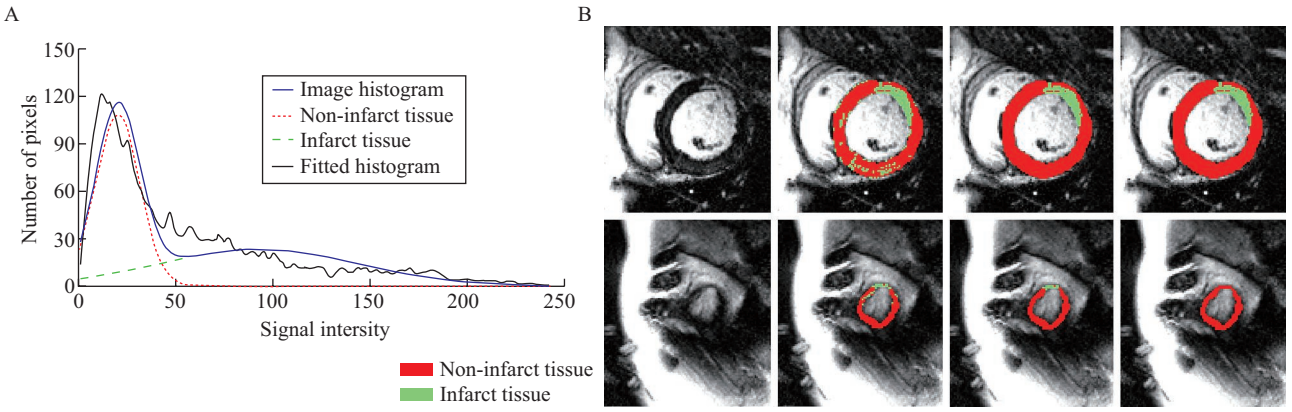

Fig. 1 Tissue classification example of LGE-MRI scanned from one human heart into two categories which are non-infarct tissue and infarct tissue by using the GMM method

images, the Dice and volume difference metrics were used to evaluate the segmentations. The Dice score represents the overlap between the ground truth (the segmentation of infarct tissue performed by two experts with more than 10 years of CMR image segmentation experience) and the segmentation generated by the automatic algorithm used in this study. It is defined as follows:

$$\text{Dice}=\frac{2(A\cap M)}{A+M}$$

where A and M denoted automatic algorithm and manually segmented regions, respectively.

2 RESULTS

The segmentation results with the automatic algorithm proposed in this paper were compared with the consensus ground truth. Figure 1A shows the tissue classification example of LGE-MRI scanned from one human heart into two categories which are non-infarct tissue and infarct tissue using the GMM method. The first column of fig. 1B shows two slices of the original human LGE-MRI. The second column shows the tissue classification results using the GMM method with two categories. The third column shows the segmentation results after applying step 2 in the method section, most of the artifacts are removed. The fourth column shows the segmentation results after applying step 3, this step moves the small clusters of pixels which are artifacts formed by fat or blood pool in the apex or base.

Figure 2 shows the segmentation accuracy measured by the Dice metric from different image sources. We divided the image sources into three different categories: the public dataset including 3 human and 5 porcine MRI scans, Anzhen_Zhengda dataset including 52 human MRI scans, and the whole dataset including the public and Anzhen_Zhengda dataset. The three individual Dice overlaps were as follows: All=0.79, Public=0.83, Anzhen_Zhengda=0.79.

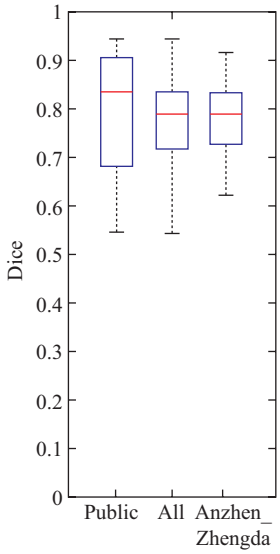

Fig. 2 Segmentation accuracy on 3 different datasets using the GMM method with two categories
The public dataset includes 3 human and 5 porcine hearts. The Anzhen_Zhengda dataset includes 52 human hearts, and all datasets include the public and Anzhen_Zhengda dataset.

Figure 3 shows the segmentation results of another human heart by GMM-based classification method with two and three categories. The first row of figure 3 shows four slices of the original human LGE-MRI. The second and third rows show the tissue classification results using the GMM method with three and two categories, respectively. For the GMM method with two categories, we applied step 4 in the method section to further divide the infarct region into gray zone and core scar. We changed the threshold value in the fourth step from 10% to 50% with an interval of 5%, and we found that 30% was the best value for infarct tissue segmentation compared with the GMM method with three categories. The fourth row of fig. 3 shows the final segmentation after applying step 4.

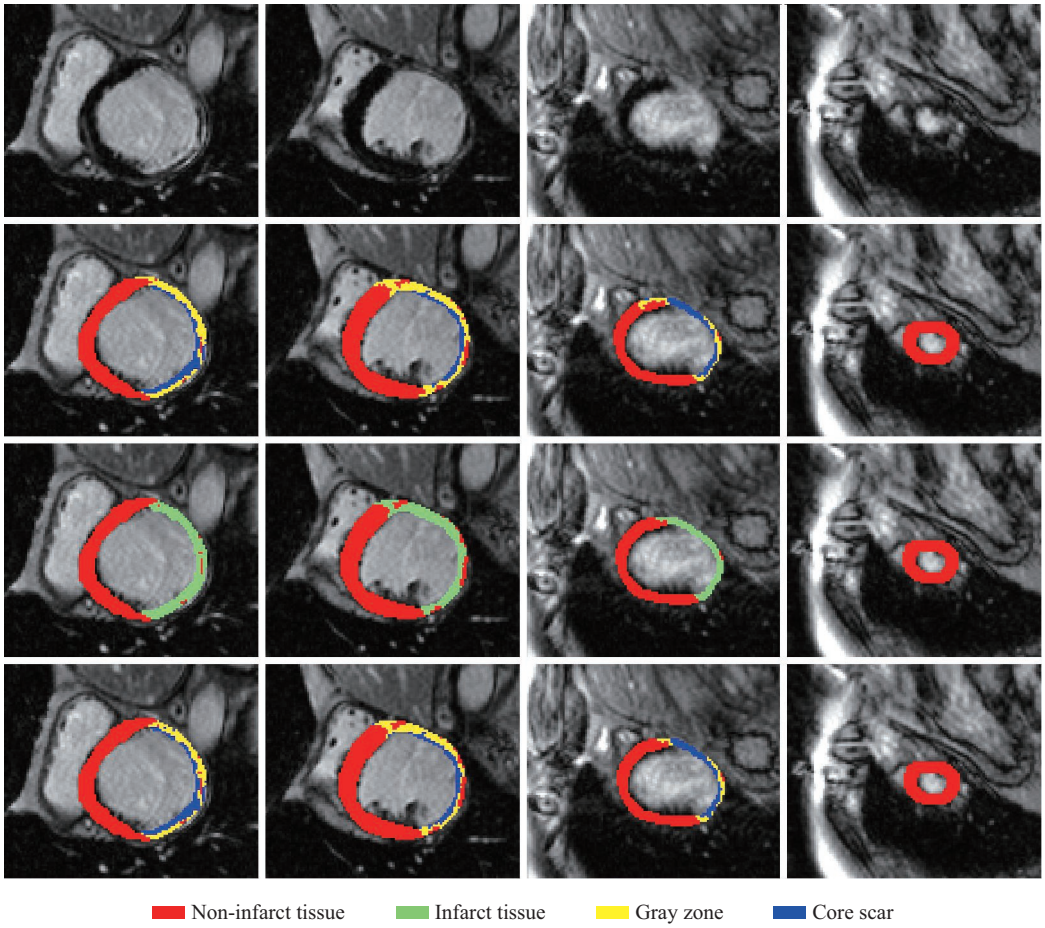

Fig. 3 Segmentation results of the LGE-MRI scanned from a human heart by GMM-based classification method with two and three categories

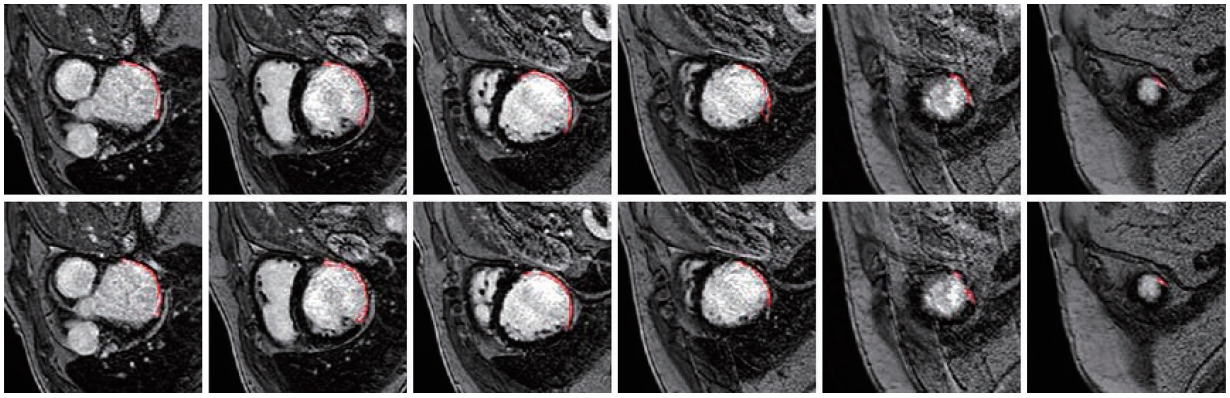

Fig. 4 Example segmentation of one human heart with low image resolution from the public dataset
The first row shows the consensus segmentation, and the second row shows the segmentation with our method.

Figures 4–5 and supplemental figures 1–2 showed detailed segmentation results of our proposed method in 3 patients and 1 porcine MRI scans. Supplemental figure 1 shows the segmentation result of one patient with high image resolution of 0.625×0.625×2 mm from the public dataset; the median value of Dice overlaps of these MRI scans was 0.94. The scar tissue segmented by our method was very close to the consensus ground truth. Figure 4 shows the segmentation result of another patient from the public dataset with low image resolution of 1.367×1.367×8 mm; the median value of Dice overlaps of these MRI scans was 0.73. We checked the scar segmentation in the consensus ground truth, and found that some pixels with low gray values were regarded as scar, and hence the Dice value was relatively lower than the high-resolution images. Supplemental figure 2 shows the segmentation results of one porcine heart from the public dataset with an image resolution of 1.718×1.718×6 mm. The median value of Dice overlaps of these MRI scans was

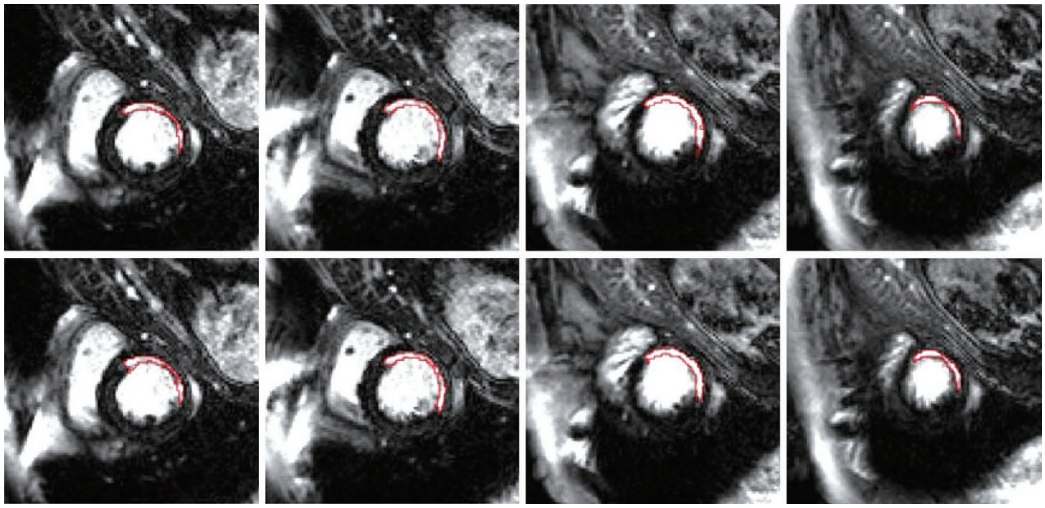

Fig. 5 Example segmentation of one human heart with low image resolution from Anzhen Hospital
The first row shows the consensus segmentation, and the second row shows the segmentation with our method.

0.92. The pixels of the scar detected by our method match well with the consensus ground truth. Figure 5 shows the segmentation results of one patient from Anzhen_Zhengda dataset with image resolution of 1.367×1.367×9.6 mm. The median value of Dice overlaps of these MRI scans was 0.88. The scar boundaries detected by our method were similar to the consensus ground truth in each slice.

3 DISCUSSION

We proposed a method to automatically detect the scar in CMR-LGE images. After segmenting the boundary of left ventricle, the subsequent processing pipeline was fully automatic without manual work. Our method is robust to different MRI sources which were scanned by different centers with different image collection parameters. The in-plane resolution of different MRI scans varies from 0.63 mm to 1.87 mm and the out-of-plane image resolution from 2 mm to 9.6 mm.

The three categories classification divided the left ventricle myocardium into non-infarct tissue, gray zone and core scar. The two categories classification divided the left ventricle myocardium into non-infarct tissue and infarct tissue which included gray zone and core scar. For the non-infarct tissue segmentation, there is very minor difference between the two and three categories classification. The only major difference between the two and three categories classification was the infarct area. For the three categories classification, the gray zone (yellow color in fig. 3) and core scar (blue color in fig. 3) were different tissues. But for the two categories classification, the gray zone and core scar were merged into one tissue which was commonly classified as infarct tissue (green color in fig. 3). Numerous methods had been published to segment the infarct tissue in the left ventricle[14, 19, 20], including manual, semi-automatic and fully automatic method, and most of these methods were used to predict the whole infarct area, which were the same as the two categories classification used in this paper. The reason that they didn't divide the infarct area into gray zone and core scar was that there was lack of experimental evidence to validate the accuracy of the LGE-MRI in segmenting gray zone and core scar. So far as we know, only a few published articles intended to segment the infarct area into gray zone and core scar with histopathology validation[18, 19]. Although the results in these papers demonstrated that the comparison between gray zone and core scar extent in LGE with the corresponding areas identified in histology yielded good correlations, we should notice that the late gadolinium-enhancement MRI was obtained from *ex-vivo* hearts. The *ex-vivo* images had very high spatial resolution compared with clinical images (0.6 mm *vs.* 1.7 mm in-plane spatial resolution, 0.6 mm *vs.* 10 mm out of plane spatial resolution), thus this method should be validated to apply it to the clinical image segmentation. So far as we know, no published literature directly compared gray zone and core scar obtained from clinic LGE-MRI with histopathology which is recognized as the golden standard widely. Thus, a few studies used computational modeling to indirectly validate the segmentation of gray zone and core scar obtained from the LGE-MRI[21, 22]. They defined the optimal range of infarct tissue threshold values to divide it into gray zone and core scar, and these threshold values provided best match between simulation and experimental/clinic results.

The main reasons we used two and three categories of calcification are that: 1) To get direction comparison of the infarct tissue segmented by the GMM-based classification method with two categories with the consensus ground truth; 2) To get indirect

comparison of the gray zone and core scar segmented by the GMM-based classification method with three categories. Owning to the main work of this paper is image segmentation, we didn't do computation modeling to validate the accuracy of the three categories of calcification. Thus, we used the same idea of other publications of computational modeling to divide the infarct area into gray zone and core scar using threshold value method. Then we compared the segmentation results with the results segmented by GMM-based classification method with three categories, which was validated using *ex-vivo* swine hearts. This indirectly validates the segmentation of gray zone and core scar obtained from the LGE-MRI with computational modeling and clinical measurements is beyond the scope of this paper.

The second step is used to remove the pixels composed of fat tissue or artifacts, which contain many pixels. The threshold value of maximal components can be adjusted too. We used a threshold of 50% in this study. If this value is low, some big artifacts will be included, especially the near-apex or base region. The third step is used to remove some small clusters of pixels formed by noises or blood vessels in some image slices which didn't contain any infarct tissue. The value used in this step can be adjusted and we find that 15 pixels are suitable for the dataset.

We used different datasets to validate the efficiency of our method. The dice value of public datasets is slightly higher than that of the Anzhen_ Zhengda dataset, and the variance is higher in the public dataset. The highest Dice value is from the images with resolution of 0.625 mm, the image quality is much better than that of the other clinical images. For the Anzhen_Zhengda dataset, the Dice value is close to that of the public dataset, and the volume difference is relatively low too, thus these results show that our method is relatively robust for different image sources.

Several automatic or semi-automatic methods have been used to segment infarct tissue, which are compared in detail in reference[14]. Those method used 30 datasets (20 for testing and 10 for training) for validation. For the validation in our study, we selected 8 datasets from their training dataset and 52 from Anzhen_Zhengda Hospital. The Dice value in the 8 public datasets is close to or better than that of the methods listed in the reference (best Dice value of 0.85 with MCG method in human datasets, and 0.86 with AIT method in the pig datasets). The Dice values in all the datasets used in this paper are close too, with a median value of 0.79. The advantage of our method compared with most of the methods listed in the reference[14] is that our method is fully automatic without requirement of manual work. This advantage is desirable when a large number of patients are involved.

Recently, the convolutional neural network method has been used for left ventricle scar segmentation, showing superior performance to conventional methods[20]. This method still needs further testing under a variety of conditions, such as a much larger cohort of patient images, or different image-scanning machines, image qualities, and image scanning parameters.

This study has several limitations. First, it was tested only in a small cohort of public datasets. If possible, we will collect more datasets from different centers scanned with different machines and different scan parameters. Second, our method may include some false segmentation which may be introduced by noise, fat tissue or artifacts from implantable cardioverter defibrillator. Third, although our method is fully automatic for scar segmentation, it still needs manual segmentation of endocardium and epicardium in the left ventricle.

In conclusion, we propose a method to automatically detect the scar in CMR-LGE images. After segmenting the boundary of left ventricle, the subsequent process pipeline is fully automatic without manual work. The results show that our method is efficient to different MRI sources which were scanned by various centers with different image collection parameters. Our segmentation accuracy is comparable to other conventional methods which are semi-automatic, indicating the efficacy of our method for processing a large number of patients in clinical use.

Conflict of Interest Statement

The authors declare that there is no conflict of interest related to the contents of this article.

REFERENCES

1 Writing Group Members; Mozaffarian D, Benjamin EJ, *et al*. Executive Summary: Heart Disease and Stroke Statistics--2016 Update: A Report From the American Heart Association. Circulation, 2016,133(4):447-454

2 Alexandre J, Saloux E, Dugué AE, *et al*. Scar extent evaluated by late gadolinium enhancement CMR: a powerful predictor of long term appropriate ICD therapy in patients with coronary artery disease. J Cardiovasc Magn Reson, 2013,15(1):2

3 West AM, Kramer CM. Cardiovascular magnetic resonance imaging of myocardial infarction, viability, and cardiomyopathies. Curr Probl Cardiol, 2010,35(4): 176-220

4 Schelbert EB, Wong TC. Imaging the area at risk in myocardial infarction with cardiovascular magnetic resonance. J Am Heart Assoc, 2014,3(4):e001253

5 Schelbert EB, Hsu LY, Anderson SA, *et al*. Late gadolinium-enhancement cardiac magnetic resonance identifies postinfarction myocardial fibrosis and the border zone at the near cellular level in ex vivo rat heart. Circ Cardiovasc Imaging, 2010,3(6):743-752

6 Perez-David E, Arenal A, Rubio-Guivernau JL, *et al*. Noninvasive identification of ventricular tachycardia-related conducting channels using contrast-enhanced magnetic resonance imaging in patients with chronic

myocardial infarction comparison of signal intensity scar mapping and endocardial voltage mapping. J Am Coll Cardiol, 2011,57(2):184-194
7 Fernández-Armenta J, Berruezo A, Andreu D, *et al*. Three-Dimensional Architecture of Scar and Conducting Channels Based on High Resolution ce-CMR: Insights for Ventricular Tachycardia Ablation. Circ Arrhythm Electrophysiol, 2013,6(3):528-537
8 Deng D, Prakosa A, Shade J, *et al*. Characterizing Conduction Channels in Postinfarction Patients Using a Personalized Virtual Heart. Biophys J, 2019,117(12): 2287-2294
9 Prakosa A, Arevalo HJ, DENG D, *et al*. Personalized virtual-heart technology for guiding the ablation of infarct-related ventricular tachycardia. Nat Biomed Eng, 2018,2(10):732-740
10 Deng D, Prakosa A, Shade J, *et al*. Sensitivity of Ablation Targets Prediction to Electrophysiological Parameter Variability in Image-Based Computational Models of Ventricular Tachycardia in Post-infarction Patients. Front Physiol, 2019,10:628
11 Prakosa A, Malamas P, Zhang S, *et al*. Methodology for image-based reconstruction of ventricular geometry for patient-specific modeling of cardiac electrophysiology. Prog Biophys Mol Bio, 2014,115(2-3):226-234
12 Amado LC, Gerber BL, Gupta SN, *et al*. Accurate and objective infarct sizing by contrast-enhanced magnetic resonance imaging in a canine myocardial infarction model. J Am Coll Cardiol, 2004,44(12):2383-2389
13 Flett AS, Hasleton J, Cook C, *et al*. Evaluation of Techniques for the Quantification of Myocardial Scar of Differing Etiology Using Cardiac Magnetic Resonance. JACC Cardiovasc Imaging, 2011,4(2):150-156
14 Karim R, Bhagirath P, Claus P, *et al*. Evaluation of state-of-the-art segmentation algorithms for left ventricle infarct from late Gadolinium enhancement MR images. Med Image Anal, 2016,30:95-107
15 Carminati MC, Boniotti C, Fusini L, *et al*. Comparison of Image Processing Techniques for Nonviable Tissue Quantification in Late Gadolinium Enhancement Cardiac Magnetic Resonance Images. J Thorac Imaging, 2016,31(3):168-176
16 Liu D, Ma X, Liu J, *et al*. Quantitative analysis of late gadolinium enhancement in hypertrophic cardiomyopathy: comparison of diagnostic performance in myocardial fibrosis between gadobutrol and gadopentetate dimeglumine. Int J Cardiovasc Imaging, 2017,33(8):1191-1200
17 Hennemuth A, Friman O, Huellebrand M, *et al*. Mixture-Model-Based Segmentation of Myocardial Delayed Enhancement MRI, Berlin, Heidelberg, F, 2013 [C]. Springer Berlin Heidelberg.
18 Pop M, Ghugre NR, Ramanan V, *et al*. Quantification of fibrosis in infarcted swine hearts by *ex vivo* late gadolinium-enhancement and diffusion-weighted MRI methods. Phys Med Biol, 2013,58(15):5009-5028
19 Rutherford SL, Trew ML, Sands GB, *et al*. High-Resolution 3-Dimensional Reconstruction of the Infarct Border Zone Impact of Structural Remodeling on Electrical Activation. Circ Res, 2012,111(3):301-311
20 Zabihollahy F, White JA, Ukwatta E. Convolutional neural network-based approach for segmentation of left ventricle myocardial scar from 3D late gadolinium enhancement MR images. Med Phys, 2019,46(4):1740-1751
21 Deng DD, Nikolov P, Arevalo HJ, *et al*. Optimal contrast-enhanced MRI image thresholding for accurate prediction of ventricular tachycardia using ex-vivo high resolution models. Comput Biol Med, 2018,102:426-432
22 Ng J, Jacobson JT, Ng JK, *et al*. Virtual electrophysiological study in a 3-dimensional cardiac magnetic resonance imaging model of porcine myocardial infarction. J Am Coll Cardiol, 2012,60(5):423-430

(Received Feb. 1, 2020; accepted Oct. 21, 2020)